SOILS AND FOUNDATIONS Vol. 25, No. 3, 41-48, Sept. 1985
Japanese Society of Soil Mechanics and Foundation Engineering

THREE-DIMENSIONAL STABILITY ANALYSIS OF VERTICAL COHESIVE SLOPES

KEIZO UGAI*

ABSTRACT

This paper presents a stability analysis of vertical cohesive slopes with a finite length (perpendicular to cross sections of slopes). The method of analysis is based on three-dimensional limit equilibrium techniques and variational calculus. The shapes of three-dimensional critical failure surfaces were determined exactly and found to be split cylinders with curved end caps. Then the three-dimensional factors of safety were calculated as the functions of the ratio of failure length to vertical slope height. These factors of safety were higher than the two-dimensional factors as indicated by Baligh and Azzouz (1975), etc. The method of analysis of this study could be extended to any inclined cohesive slope. The solutions obtained here give the least upper bound of the problem in limit analysis. In practice they can be applied to evaluate the end effects of vertical cuts or excavations in clays in narrow areas.

Key words : cut slope, excavation, safety factor, slope stability, stability analysis (**IGC** : E 6)

INTRODUCTION

In many cases, problems of slope stability are analyzed two-dimensionally, assuming plane-strain conditions. However, the failure regions of actual slopes have finite dimensions, so a 3-D (three-dimensional) approach is needed to analyze their failure mechanism accurately. Lefebvre, Duncan and Wilson (1973) and Baligh and Azzouz(1975) indicate that the 3-D (end) effect is important for the problem of stability of dams in steep-walled valleys.

Baligh and Azzouz(1975) analyze the 3-D stability of cohesive slopes by extending the circular arc method, assuming two types of failure surfaces : split cylinders with conical ends or with elliptical ends. They show that the end effects give 4%-40% higher values than the 2-D (two-dimensional) factor of safety.

Hovland(1977) presents the 3-D method of analysis for slopes of c-ϕ soils with various shapes of failure surfaces by extending the 2-D slice method. He also offers an interesting conclusion, stating that some situations exist where 3-D factors of safety can be lower than 2-D factors of safety in sandy slopes.

Azzouz, Baligh and Ladd (1981) present four case histories of embankments rapidly loaded to failure on saturated clay foundations. They show that end effects increase the conventional two-dimensional factor of safety by as much as 30%, and hence, if neg-

* Associate Professor, Gunma University, 1 Tenjin-cho, Kiryu, Gunma.
Manuscript was received for review on September 27, 1984.
Written discussions on this paper should be submitted before April 1, 1986, to the Japanese Society of Soil Mechanics and Foundation Engineering, Sugayama Bldg. 4 F, Kanda Awaji-cho 2-23, Chiyoda-ku, Tokyo 101, Japan. Upon request the closing date may be extended one month.

lected, can lead to significant overestimation of backfigured strengths.

Chen and Chameau(1982) present a new method of 3-D stability analysis for rotational failure surfaces which is an extension of Spencer's slice method in the 2-D problems. They also present the 3-D finite element method of slope stability analysis, which gives almost the same results as their 3-D slice method.

As stated above, there have been several new methods presented which lead to some interesting and important conclusions regarding 3-D slope stability problems. However, many problems still remain to be solved, such as the determination of the critical 3-D failure surface, the evaluation of minimum safety factors, and so on.

The object of this study is to present a new method of analysis which makes it possible to determine the critical failure surface and to evaluate exactly the 3-D effects on the safety factor by use of variational calculus. This variational method has been used in several slope stability analyses. This method will be a powerful tool for slope stability analysis if the well-known Euler's differential equation can be solved exactly or numerically, because this would make it unnecessary to investigate a great number of trial circular or non-circular failure surfaces and to make tedious calculations.

3-D CRITICAL FAILURE SURFACE OF COHESIVE SLOPES

Fig. 1(a) shows a cohesive slope with angle β and its assumed 3-D failure surface. The

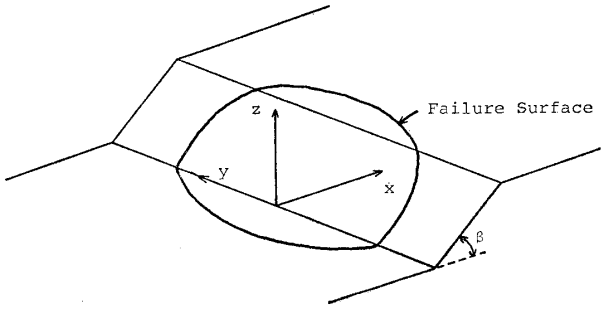

(a) **3-D failure surface**

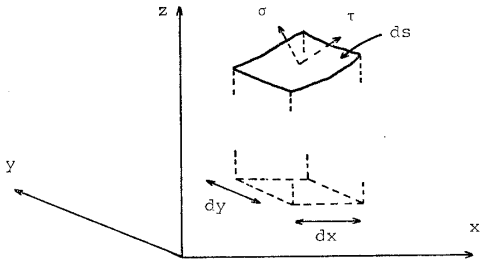

(b) **Infinitesimal element of failure surface**

Fig. 1. 3-D failure surface and its infinitesimal element

y-coordinates of both ends of the failure surface are given by $y=\pm L$ (L : constant). The sliding direction of the mass is assumed to be perpendicular to the y-axis. The shape of the 3-D failure surface is considered to be symmetrical with respect to the plane $y=0$. The area ds of an infinitesimal element of the failure surface, the projection of which on the plane $z=0$ is a rectangle with the area $dx \cdot dy$ (Fig. 1(b)), is given as follows :

$$ds=\sqrt{1+\left(\frac{\partial z}{\partial x}\right)^2+\left(\frac{\partial z}{\partial y}\right)^2}\,dxdy=\Delta dxdy \quad (1)$$

where $\Delta=\sqrt{1+\left(\frac{\partial z}{\partial x}\right)^2+\left(\frac{\partial z}{\partial y}\right)^2}$ and $z(x, y)$ is the equation of the failure surface. The unit vector normal to ds is given by

$$\left(-\frac{\partial z}{\partial x}\Big/\Delta,\ -\frac{\partial z}{\partial y}\Big/\Delta,\ 1/\Delta\right) \quad (2)$$

This unit vector also shows the direction of the normal stress $\sigma(x, y)$ on ds.

The shear stress τ on the failure surface is defined as follows :

$$\tau=c/F \quad (3)$$

where c is the cohesion and F is the safety factor. Since the sliding direction is limited in the xz-plane, the direction of the force τds is given by the following unit vector :

$$\left(1/\Delta',\ 0,\ \frac{\partial z}{\partial x}\Big/\Delta'\right) \quad (4)$$

where

$$\Delta'=\sqrt{1+\left(\frac{\partial z}{\partial x}\right)^2} \quad (5)$$

Now we can obtain the equations of horizontal, vertical and moment equilibrium for

the sliding mass as follows :

$$\int\left(\tau/\Delta'-\sigma\frac{\partial z}{\partial x}\Big/\Delta\right)ds=0 \qquad (6)$$

$$\int\left(\tau\frac{\partial z}{\partial x}\Big/\Delta'+\sigma/\Delta\right)ds-\iint\gamma(\bar{z}-z)\,dxdy=0 \qquad (7)$$

$$\int\left(\tau/\Delta'-\sigma\frac{\partial z}{\partial x}\Big/\Delta\right)zds-\int\left(\tau\frac{\partial z}{\partial x}\Big/\Delta'+\sigma/\Delta\right)xds+\iint\gamma x(\bar{z}-z)\,dxdy=0 \qquad (8)$$

where γ is the unit weight of soil and $\bar{z}(=\bar{z}(x, y))$ is the equation of the slope surface.

It is convenient to introduce the following non-dimensional quantities : $N=c/\gamma H$, $S=\sigma/\gamma H$, $X=x/H$, $Y=y/H$, $Z=z/H$, where H is the height of the slope, in accordance with Baker and Garber (1977). Substituting Eqs. (1) and (3) into Eqs. (6), (7) and (8), we obtain the following equilibrium equations :

$$\iint\left(N\Delta/\Delta'-FS\frac{\partial Z}{\partial X}\right)dXdY=0 \qquad (9)$$

$$\iint\left[N\frac{\partial Z}{\partial X}\Delta/\Delta'-F(\bar{Z}-Z-S)\right]dXdY=0 \qquad (10)$$

$$\iint\left[N\left(Z-\frac{\partial Z}{\partial X}X\right)\Delta/\Delta'-F\left\{S\left(X+\frac{\partial Z}{\partial X}Z\right)-X(\bar{Z}-Z)\right\}\right]dXdY=0 \qquad (11)$$

In this section the problem is to determine the functions $Z(X, Y)$ and $S(X, Y)$ which minimize the safety factor F, and this problem will be solved using variational calculus. The only restriction is that the functions Z and S are continuous and differentiable.

Following the methods of formulation by Baker and Garber (1977), and referring to Elsgolc (1962), the functions Z and S which minimize F must satisfy the following Ostrogradski (Euler-Lagrange's) partial differential equations :

$$\frac{\partial}{\partial Y}\left(\frac{\partial G}{\partial S_Y}\right)+\frac{\partial}{\partial X}\left(\frac{\partial G}{\partial S_X}\right)-\frac{\partial G}{\partial S}=0 \qquad (12)$$

$$\frac{\partial}{\partial Y}\left(\frac{\partial G}{\partial Z_Y}\right)+\frac{\partial}{\partial X}\left(\frac{\partial G}{\partial Z_X}\right)-\frac{\partial G}{\partial Z}=0 \qquad (13)$$

where

$$G=\left(N\Delta/\Delta'-FS\frac{\partial Z}{\partial X}\right)+\lambda_1\left\{N\frac{\partial Z}{\partial X}\Delta/\Delta'-F(\bar{Z}-Z-S)\right\}+\lambda_2\left[N\left(Z-\frac{\partial Z}{\partial X}X\right)\Delta/\Delta'-F\left\{S\left(X+\frac{\partial Z}{\partial X}Z\right)-X(\bar{Z}-Z)\right\}\right] \qquad (14)$$

$$S_X=\frac{\partial S}{\partial X},\quad S_Y=\frac{\partial S}{\partial Y},\quad Z_X=\frac{\partial Z}{\partial X},\quad Z_Y=\frac{\partial Z}{\partial Y}$$

and λ_1, λ_2 are constants called Lagrange's multipliers. Since $\frac{\partial G}{\partial S_{X,Y}}=0$, we can obtain the following first-order differential equation of $Z(X, Y)$, from Eq. (12) and (14) :

$$(1+\lambda_2 Z)\frac{\partial Z}{\partial X}+\lambda_2 X-\lambda_1=0 \qquad (15)$$

Solving Eq. (15), we obtain

$$(Z-Z_c)^2+(X-X_c)^2=R^2(Y) \qquad (16)$$

where $Z_c=-1/\lambda_2$, $X_c=\lambda_1/\lambda_2$ and $R(Y)$ is an arbitrary function of Y. Eq. (16) represents the surface of a rotational body whose axis is expressed by the coordinate (X_c, Z_c) in the XZ-plane.

Substituting $Z(X, Y)$ from Eq. (16) into Eq. (13), we can obtain the differential equation of S.

FOR THE CASE OF VERTICAL COHESIVE SLOPES

In the discussion of the previous section, it was proved that the 3-D critical failure surface of any inclined cohesive slope is the surface of a rotational body, in the sense of the limit equilibrium. In this section we limit the discussion to vertical ($\beta=90°$) cohesive slopes.

Figs. 2(a) and (b) show a vertical cohesive slope and its assumed failure surface. The failure surface is assumed to be composed of three parts :

(1) a cylinder passing through the toe ($R(y)=R_0$: constant) ; (2)curved end caps similar to ellipsoids ($R(y)$: variable) ; and (3) sectors of a circle perpendicular to the y-axis (Fig. 2(a)). Part (1) is assumed, since if $L\to\infty$, the critical surface approaches an infinite cylinder passing through the toe. Part (3) is assumed since it makes the safety fac-

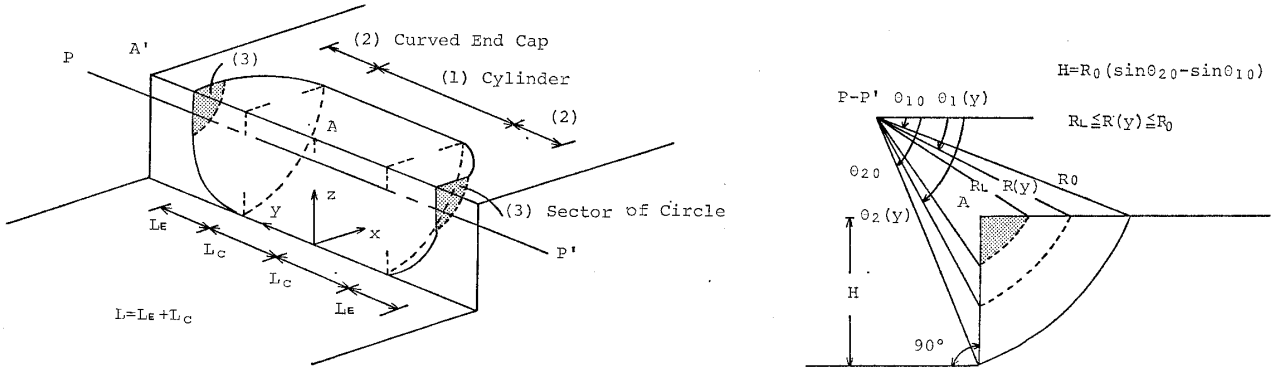

(a) **Three parts of failure surface** (b) **Section of vertical slope**

Fig. 2. 3-D failure surface of vertical slope

tor lower than in the case where it is not assumed.

In Figs. 2(a) and (b), P-P' is the axis of rotation of the failure surface. $\theta_1=\theta_1(y)$ and $\theta_2=\theta_2(y)$ express both ends of the cross section of the failure surface, and $R=R(y)$ is the radius. In the following discussions we will consider the half$(0\leqq y\leqq L)$ of the failure surface, since it is symmetrical with respect to the plane $y=0$.

The resisting moment M_r is expressed as follows :

$$M_r=\frac{c}{F}\int_0^L \{\theta_2(y)-\theta_1(y)\}\{R(y)\}^2 \times\sqrt{1+\{R'(y)\}^2}dy=M_{r1}+M_{r2}+M_{r3} \tag{17}$$

where M_{r1}, M_{r2} and M_{r3} are the resisting moments of parts (1), (2) and (3), respectively, which are given by

$$M_{r1}=\frac{c}{F}\int_0^{L_c}(\theta_{20}-\theta_{10})R_0^2dy =\frac{c}{F}(\theta_{20}-\theta_{10})R_0^2L_c \tag{18.1}$$

$$M_{r2}=\frac{c}{F}\int_0^{L_E}\{\theta_2(y_E)-\theta_1(y_E)\}\{R(y_E)\}^2 \times\sqrt{1+\{R'(y_E)\}^2}dy_E \tag{18.2}$$

$$M_{r3}=\frac{c}{F}\int_{R_m}^{R_L}\{\theta_2(L)-\theta_1(L)\}\{R(L)\}^2dR =\frac{c}{F}\int_{R_m}^{R_L}\left\{\cos^{-1}\left(\frac{a}{R}\right)-\sin^{-1}\left(\frac{b}{R}\right)\right\}R^2dR \tag{18.3}$$

where

$$\left.\begin{aligned}&\sin\theta_1(y)=\frac{R_0}{R(y)}\sin\theta_{10},\\&\cos\theta_2(y)=\frac{R_0}{R(y)}\cos\theta_{20}\\&a=R_0\cos\theta_{20},\quad b=R_0\sin\theta_{10},\quad y_E=y-L_c\end{aligned}\right\} \tag{18.4}$$

R_0 is the distance between the axis P-P' and the toe.

θ_{10} and θ_{20} are the values of θ_1 and θ_2 of the toe circle, respectively.

L_c is the length of the part of the cylinder.

L_E is the length of the part of the end cap.

R_m is the distance between the axis P-P' and the point A (Figs. 2(a), (b)).

R_L is the radius of the boundary arc of part (2).

The driving moment M_d is expressed as follows (Chen, 1975) :

$$M_d=\frac{\gamma}{6}\int_0^{L_c+L_E}\{R(y)\}^3\{\sin\theta_2(y)-\sin\theta_1(y)\}^2 \times\{2\sin\theta_2(y)+\sin\theta_1(y)\}dy=M_{d1}+M_{d1} \tag{19}$$

where

$$M_{d1}=\frac{\gamma}{6}R_0^3(\sin\theta_{20}-\sin\theta_{10})^2 \times(2\sin\theta_{20}+\sin\theta_{10})L_c \tag{20.1}$$

$$M_{d2}=\frac{\gamma}{6}\int_0^{L_E}\{R(y_E)\}^3\{\sin\theta_2(y_E)-\sin\theta_1(y_E)\}^2 \times\{2\sin\theta_2(y_E)+\sin\theta_1(y_E)\}dy_E \tag{20.2}$$

The moment equilibrium about the axis P-P' is

$$M_r=M_d \tag{21}$$

From Eqs. (20) and (21), the safety factor F and the stability factor N_s are given as follows :

$$N_s=\frac{\gamma HF}{c}=\frac{\{FM_r/c\}}{\{M_d/(\gamma H)\}} \tag{22}$$

$$\{FM_r/c\}=\int_0^{L_E}[H_1+\{\theta_2(y_E)-\theta_1(y_E)\}\times\{R(y_E)\}^2\sqrt{1+\{R'(y_E)\}^2}+H_2]dy_E \tag{23.1}$$

$$\{M_d/(\gamma H)\}=\int_0^{L_E}\Big[H_3+\frac{1}{\sigma H}\{R(y_E)\}^3\times\{\sin\theta_2(y_E)-\sin\theta_1(y_E)\}^2\times\{2\sin\theta_2(y_E)+\sin\theta_1(y_E)\}\Big]dy_E \tag{23.2}$$

where

$$H_1=\frac{F}{c}M_{r1}/L_E=(\theta_{20}-\theta_{10})R_0^2\frac{L_c}{L_E} \tag{23.3}$$

$$H_2=\frac{F}{c}M_{r3}/L_E=\frac{1}{L_E}\int_{Rm}^{RL}\left\{\cos^{-1}\left(\frac{a}{R}\right)-\sin^{-1}\left(\frac{b}{R}\right)\right\}R^2dR \tag{23.4}$$

$$H_3=\frac{M_{d1}}{\gamma H}\Big/L_E=\frac{R_0{}^3L_c}{6HL_E}(\sin\theta_{20}-\sin\theta_{10})^2\times(2\sin\theta_{20}+\sin\theta_{10}) \tag{23.5}$$

Therefore the problem is reduced to one of the variational method in which N_s is minimized with respect to the function R. Noting that H_1, H_2 and H_3 are constants, Euler's differential equation is given by (Baker and Garber, 1977)

$$\frac{d}{dy_E}\left\{\frac{\partial}{\partial R'}(f\sqrt{1+R'^2}-N_sg)\right\}-\frac{\partial}{\partial R}(f\sqrt{1+R'^2}-N_sg)=0 \tag{24}$$

where

$$f=\{\theta_2(R)-\theta_1(R)\}R^2 \tag{24.1}$$

$$g=\frac{R^3}{6H}\{\sin\theta_2(R)-\sin\theta_1(R)\}^2\times\{2\sin\theta_2(R)+\sin\theta_1(R)\} \tag{24.2}$$

From Eq. (24) we obtain the following second-order differential equation of $R(y_E)$:

$$R''+\frac{(1+R'^2)^{3/2}}{f}\left(-\frac{\partial f}{\partial R}\Big/\sqrt{1+R'^2}+N_s\frac{\partial g}{\partial R}\right)=0 \tag{25}$$

This differential equation is easily solved if $t=1/\sqrt{1+p^2}$ and $R''=\frac{1}{2}\frac{dp^2}{dR}\left(p=\frac{dR}{dy_E}\right)$ are substituted into Eq. (25). After some calculations, we obtain

$$\frac{1}{\sqrt{1+p^2}}=\frac{1}{f}(N_sg+C) \tag{26}$$

where C is an integral constant. If it is assumed that R and $R'(=p)$ are continuous at $Y_E=0$ (where $y=L_c$ and $R=R_0$), p must be zero at $Y_E=0$ or $R=R_0$. Substituting $p=0$ and $R=R_0$ into Eq. (26), we obtain

$$C=f_0-N_sg_0 \tag{27}$$

where

$$f_0=(\theta_{20}-\theta_{10})R_0^2$$

$$g_0=\frac{H}{6}R_0(2\sin\theta_{20}+\sin\theta_{10})$$

Further, if it is assumed that R and R' are continuous at $y_E=L_E$ (where $y=L=L_C+L_E$, and $R=R_L$), p must be infinite at $y_E=L_E$ or $R=R_L$. Substituting $p=+\infty$, and $R=R_L$ into Eq. (26), we obtain

$$N_s\frac{g_{R=RL}}{g_0}+\frac{f_0}{g_0}-N_s=0 \tag{28}$$

Since f_0/g_0 means N_s for the two-dimensional case (that is, $L\to\infty$), Eq. (28) is expressed by

$$\frac{g_{R=RL}}{g_0}=\frac{N_s-N_{s2}}{N_s},\quad\text{where } N_{s2}=f_0/g_0 \tag{29}$$

R_L is determined by Eq. (28) or (29). From Eq. (26), we obtain

$$p=\frac{dR}{dy_E}=-\sqrt{\frac{f^2}{(N_sg+C)^2}-1} \tag{30}$$

Solving the above first-order differential equation, we obtain

$$\int_{R_0}^{R}dR\Big/\sqrt{\frac{f^2}{(N_sg+C)^2}-1}=-y_E \tag{31}$$

where the condition in which $R=R_0$ at $y_E=0$ was taken into account Eq. (31). expresses the relation between $R(y_E)$ and y_E.

Since $R=R_L$ at $y_E=L_E$, we obtain from Eq. (31)

$$L_E=-\int_{R_0}^{R_L}dR\Big/\sqrt{\frac{f^2}{(N_sg+C)^2}-1} \tag{32}$$

In this section we have limited the discussion to vertical cohesive slopes. However,

the above procedures can be extended to be applicable for any inclined cohesive slope if we can express exactly a resisting moment M_r and a driving moment M_d for the slope with angle β.

METHOD OF CALCULATIONS

The data which are needed to calculate the minimum value of N_s or F are γ, c, H, and L. Using the non-dimensional quantities as shown in the preceding section, the problem will be reduced to one that minimizes N_s for L/H only.

The procedure of calculations is as follows :

1. Assume the values of θ_{10}, θ_{20} and the initial value of N_s. Obtain R_L, $R(y_E)$ and L_E from Eqs. (28), (31) and (32), respectively. Calculate L_C from $L_C=L-L_E$. Next, substitute these values and the function $R(y_E)$ into the right-hand side of Eq. (22) and obtain the calculated N_s. Unless this calculated N_s is very close to the assumed N_s, the iteration procedure is used, until the accurate value of N_s is obtained. Thus we obtain the critical value of N_s ($(N_s)_{cri}$) corresponding to θ_{10}, θ_{20}.
2. Assume the various values of θ_{10}, θ_{20} and obtain the corresponding critical N_s in the same manner as for the above procedure.
3. From the above calculations we can determine the minimum value of N_s ($(N_s)_{min}$).

RESULTS

For the Case in which the Axis of Rotation is A-A'

Fig. 3 shows the shapes of the 3-D critical failure surfaces for $L_C/H=0.1$, 0.5, 2.0, 3.5, 5.0, which were determined by using the variational method in the case in which the axis of rotation is A-A'. In this case, $\theta_1(y)=\theta_{10}=0$ and $\theta_2(y)=\theta_{20}=\frac{\pi}{2}$. Since the curved end-cap portions of critical failure surfaces are small, their shape is relatively similar to the complete cylinder with the plane end caps, as shown in Fig. 3.

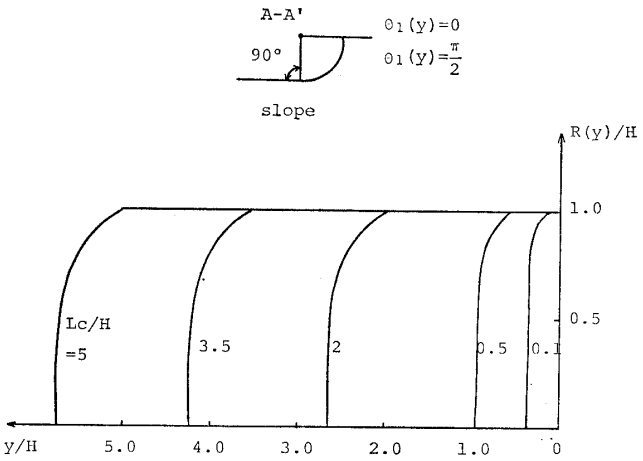

Fig. 3. 3-D critical failure surfaces in the case in which the axis of rotation is A-A'

Fig. 4 shows the relation between the half-length L of the failure surface and the 3-D critical stability factor $(N_s)_{cri}$. In this figure, L and $(N_s)_{cri}$ are divided by H and N_{s2}, respectively, where N_{s2} indicates the 2-D critical stability factor whose value is $3/2\,\pi$. In Fig. 4, the critical values of N_s for six other assumed failure surfaces are also shown : cone, ellipsoid, cylinder plus plane ends, cylinder plus cone ends, cylinder plus ellipsoidal ends, and cylinder plus cones with plane ends. From Fig. 4, it can be seen that the values of the critical 3-D stability factor obtained by the variational method are close to those of the cylinder plus plane ends and very close to those of the cylinders plus curbed end caps.

Minimum Stability Factor

As stated in the preceding section, we can determine the 3-D minimum stability factor by calculating N_s for various values of θ_{10} and θ_{20}. Fig. 5(a) shows the relation between the half-length L of failure surface and the 3-D minimum stability factor $(N_s)_{min}$ determined by the variational method. In this figure, L and $(N_s)_{min}$ are divided by H and $(N_{s2})_{min}$, respectively, where $(N_{s2})_{min}$ indicates the 2-D minimum stability factor whose value is 3.831. Fig. 5(b) shows the values of θ_{10} and θ_{20} which correspond to $(N_s)_{min}$. The minimum values of N_s for the

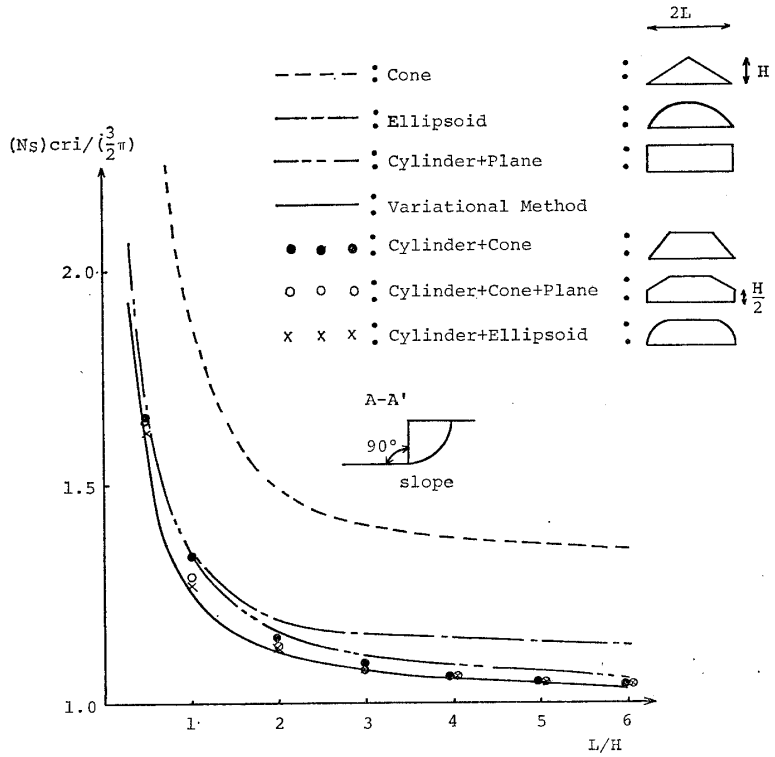

Fig. 4. 3-D critical stability factor vs. failure length in the case in which the axis of rotation is A-A'

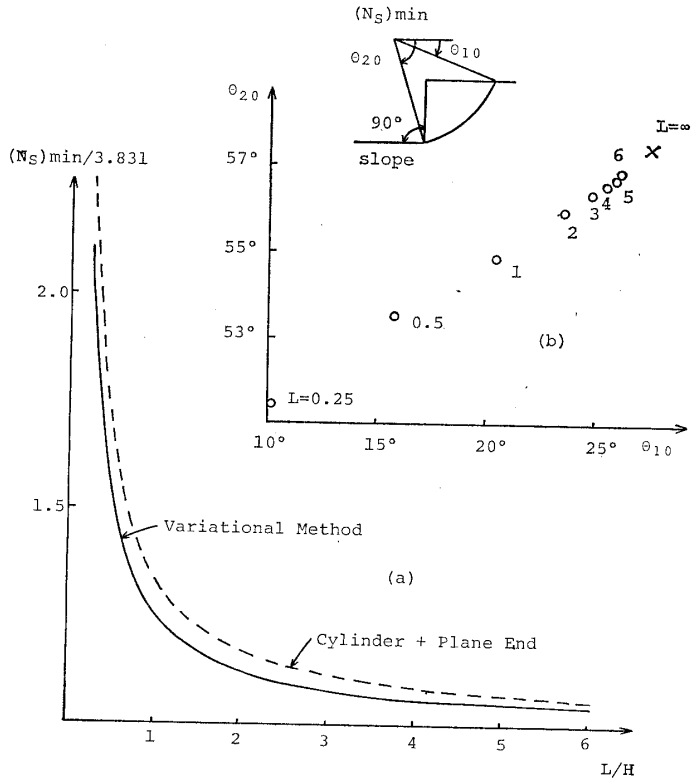

Fig. 5. (a) 3-D minimum stability factor $(N_s)_{min}$ vs. failure length, (b) θ_{10} and θ_{20} corresponding to $(N_s)_{min}$

assumed failure surface of the cylinder plus plane ends are also shown in Fig. 5(a). From Fig. 5(a) it can be seen that the $(N_s)_{min}$ determined by the variational method is approximated by the case of the cylinder plus plane ends. In practice, for example, if a vertical excavation whose width is equal to its depth is performed, its 3-D safety factor may be evaluated as about 1.5 times the 2-D safety factor by using Fig. 5(a).

CONCLUSIONS

1. By the new method of analysis based on the 3-D limit equilibrium techniques and variational calculus, the shapes of the 3-D critical failure surfaces of vertical cohesive slopes are determined exactly and found to be split cylinders with curved end caps.

2. The exact 3-D safety factors of slopes, which are calculated as functions of the ratios of slope length to vertical slope height, are higher than the 2-D safety factors indicated by former researchers.

3. The 3-D critical failure surfaces and the 3-D minimum safety factors of vertical cohesive slopes are approximated by the case of the assumed failure surfaces of cylinders plus plane ends.

REFERENCES

1) Azzouz, A. S., Baligh, M. M. and Ladd, C. C. (1981) : "Three-dimensional stability analyses of four embankment failures," Proc., 10 th ICSMFE, Vol. 3, pp. 343-346.

2) Baker, R. and Garber, M. (1977) : "Variational approach to slope stability," Proc., 9 th ICSMFE, Vol. 2, pp. 9-12.

3) Baligh, M. M. and Azzouz, A. S. (1975) : "End effects on stability of cohesive slopes," Proc., ASCE, GT 11, Vol. 101, pp. 1105-1117.

4) Chen, W. F. (1975) : Limit Analysis and Soil Plasticity, Elsevier, Amsterdam.

5) Chen, R. H. and Chameau, J. L. (1982) : "Three-dimensional slope stability analysis," Proc., 4 th International Conference on Numerical Methods in Geomechanics, Vol. 2, pp. 671-677.

6) Elsgolc, L. E. (1962) : Calculus of Variation, Pergamon Press (Japanese Edition).

7) Hovland, H. J. (1977) : "Three-dimensional slope stability analysis method," Proc., ASCE, GT 9, Vol. 103, pp. 971-986.

8) Lefebvre, G., Duncan, J. M. and Wilson, E. L. (1973) : "Three-dimensional finite element analyses of dams," Proc. ASCE, SM 7, Vol. 99, pp. 495-507.